

## Introduction

Resting state fMRI time-series data from functionally connected regions of the brain has been shown to exhibit a high degree of temporal coherence of low-frequency fluctuations ( $\leq 0.1\text{Hz}$ ). These synchronous fluctuations occur spontaneously by changes of local blood flow. In the past, researchers were able to confirm synchronous fluctuations of several structures of the motor system, auditory system, and visual system. The method to obtain functionally connected regions has been based on a temporal correlation analysis (after low-pass filtering) of pixels ("seed" pixels) in a small region of eloquent cortex with all other pixels of the brain.<sup>1-3</sup>

In this report we applied independent component analysis (ICA) to obtain spatially independent patterns in resting state fMRI time-series data as an alternative to correlation maps for functional connectivity analysis. ICA is a powerful method for the analysis of fMRI data, because it does not make assumptions about the signal intensity as a function of time or space. In activation fMRI studies, it has recently been shown that ICA can extract both transient and consistently task-related, as well as physiologically-relevant non-task-related, and various artifactual components (gross motion) of the observed fMRI signals<sup>4-6</sup>. In the near future, we intend to apply functional connectivity analysis to patients with psychiatric disorders.

## Theory

ICA assumes that the time-series data are related by a linear transformation to spatially independent components (sources), according to

$$S_{ip} = \sum_t W_{it} X_{tp}, \quad (1)$$

where  $S_{ip}$  is the  $i$ -th source of pixel  $p$ ,  $X_{tp}$  is the fMRI signal intensity of pixel  $p$  at time  $t$  where the mean signal intensity (over  $p$ ) has been subtracted, and  $W_{it}$  is the linear transformation (weighting matrix). The weighting matrix is square and of full rank. The average time course of the  $i$ -th source is given by the inverse of  $W$ , i.e.  $W_{it}^{-1}$ . The sources  $S_i$  are statistically independent of each other and thus have vanishing pairwise moments (between component  $i$  and  $i'$ ) up to all orders  $n$ , i.e.

$$\sum_p S_{ip}^n S_{i'p}^n = 0 \text{ for all } n=1,2,3,\dots,\infty, \text{ and all components } i, i'. \quad (2)$$

Independent component analysis (or blind source separation) as formulated by Comon<sup>4</sup> attempts to estimate  $W$  and  $S$  from  $X$  by minimizing the mutual information in  $S$ . Bell and Sejnowski<sup>5</sup> have proposed a neural network algorithm to obtain the ICA components.

## Methods

This research was performed on a 1.5T GE Horizon MRI scanner (Waukesha, WI) with high-speed gradients to allow EPI BOLD contrast acquisition. The EPI scanning protocol consisted of the parameters: Flip 90 deg, TE 50ms, TR 2000ms, FOV 24cm x 24cm, slice thickness 7mm, gap 2mm, 18 slices (whole brain coverage), 64 x 64 imaging matrix, 125kHz receiver bandwidth. Five healthy volunteers were studied in both resting and task-activation states.

For the resting state studies a series of 260 images were acquired in the coronal plane during which time the volunteers were instructed to refrain from any cognitive, sensory or motor activity and to keep their eyes closed. In order to identify normal functional activation patterns of motor, visual and auditory cortex, regular task activation studies were done such as bilateral finger tapping, passive listening to narrated text, verb generation, and looking at a strobe light of 8Hz frequency.

The scan protocol for the activation studies consisted of four on-off cycles, each cycle 64 sec, 148 images total, all other parameters were the same as for the resting state scans. The task-activation data were analyzed by cross correlation to a boxcar function and by ICA. Patterns of activity were identified for the motor, language, auditory and visual systems. Seed pixels in the Rolandic cortex, dentate nucleus of the cerebellum, primary auditory cortex, striate cortex, hippocampus, and Broca's area were selected in the resting state studies.

To reduce the number of noisy or irrelevant pixels, the pixel locations belonging to CSF and major arteries and veins were determined. CSF appears to be very bright on the first non-saturated EPI image and can be thresholded out. Furthermore, the location of major pulsations from larger blood vessels can be obtained from a SNR map and suppressed by thresholding. Furthermore, temporal smoothing using a 3 point Hanning filter was performed. Since each slice was collected at a different time during TR, all signal intensities of each slice were time-corrected by shifting the smoothing filter accordingly. Then, a low pass filter in the frequency domain was applied to the remaining pixel time courses to effectively remove frequencies higher than 0.1Hz. We found, that the aliased cardiac frequency, occurring in the low frequency domain, has a small amplitude for pixels in gray matter. Removing this frequency by a band-reject

filter does not improve the connectivity maps significantly. The correlation coefficients are calculated for the resting-state fluctuations between selected seed pixels in a functional region of interest and all other gray and white matter pixels in the brain, and correlation maps were prepared showing the location of all pixels with a correlation threshold exceeding 0.3.

A Blind Source Separation algorithm was applied using the extended ICA method of Bell and Sejnowski to all resting-state data in gray and white matter only. The resulting matrix size of the data was on the order of 256\*8000. The ICA components were converted to a z-score and all components were ranked according to their cumulative z-score content above the threshold  $|z|=4$ .

## Results and Discussion

Figure 1 shows the results of four different methods of data analysis. We applied a conventional t-statistic to task-activated data sets for three different experiments leading to activation in the visual cortex, auditory cortex and Broca's area. The same data sets were reanalyzed with ICA. Then, using a resting state acquisition, we applied ICA on the resting-state data as well as functional connectivity analysis via cross correlation of selected seed pixels. If the seed pixels in the cross correlation calculation are chosen carefully, we found that functional connectivity analysis in the resting state and ICA in the resting state can produce very similar patterns for visual cortex, auditory cortex, and Broca's area. We have only seen a few instances, where ICA maps are different. For example, cross correlation analysis of pixels from the primary motor cortex predicts a small but present functional connectivity to nuclei in the cerebellum, but ICA in the resting data split up these two functionally connected areas into two separate components.

Maps from resting state data as compared to activation-state data differ in general when compared across several slices, since more functional areas are involved for task execution.

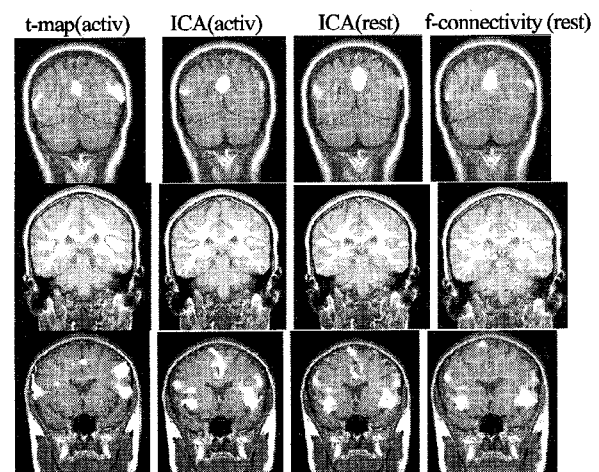


Figure 1. Activity patterns in the visual cortex (top row), primary auditory cortex (middle row), and Broca's area (bottom row) analyzed by a conventional t-statistic in a task-activation state (1. column), ICA in a task-activated state (2. column), ICA using resting state data (3. column), and functional connectivity in the resting state (4. column).

## Conclusion

Functionally related brain regions can be identified by means of their synchronous slow fluctuations in blood flow in motor cortex, SMA, expressive and receptive language regions, and limbic regions. Such blood flow synchrony can be detected also by using ICA in resting state acquisitions. For some cases however, due to sensitivity of ICA to super-Gaussian distributions, functional connectivity patterns as calculated by cross correlation methods can split into further ICA components.

## Acknowledgements

Financial support was provided by the UW-Radiology R&D fund. We like to thank Sigurd Enghoff (Technical University of Denmark) for providing the ICA package.

## References

1. Friston K.J. et al, J. Cerebral Blood Flow and Metabolism 13, 5-14 (1993).
2. Biswal B.B. et al, MRM 34, 537-541 (1995), Neuroimage 3, S305 (1996).
3. Lowe M.J. et al, Neuroimage 3, S257 (1996)+7, 119-132 (1998).
4. Comon P., Signal Processing 36, 11-20 (1994).
5. Bell AJ, Sejnowski T.J., Neural Comput., 7:1129-1159 (1995).
6. McKeown M.J. et al, Proc. Natl. Acad. Sci. 95, 803-810 (1998), HBM 6, 160-188 (1998).